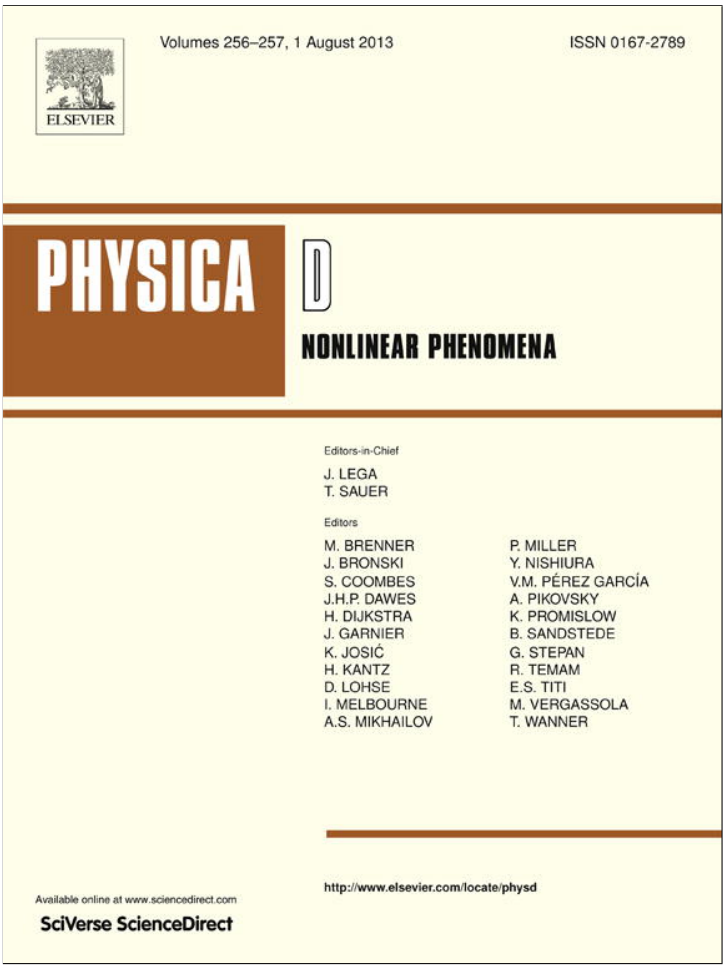

Physica D 256–257 (2013) 1–6

Contents lists available at SciVerse ScienceDirect

Physica D

journal homepage: www.elsevier.com/locate/physd

Do nonlinear waves in random media follow nonlinear diffusion equations?

T.V. Laptyeva [a,*], J.D. Bodyfelt [a], S. Flach [a,b]

[a] Max-Planck-Institut für Physik Komplexer Systeme, Dresden, Germany

[b] New Zealand Institute for Advanced Study, Massey University, Auckland, New Zealand

HIGHLIGHTS

- We study the evolution of NDE and dynamics of nonlinear disordered lattices (KG/DNLS).
- We used two key quantities: the statistical measures of second moment and kurtosis.
- The numerics show good correspondence to NDE analytics in a wide parameters range.
- We also introduced a modified NDE with long-range exponentially decaying coupling.
- Numerics for above model show even deeper correspondence of KG/DNLS and the NDE.

ARTICLE INFO

Article history:
Received 26 June 2012
Received in revised form
4 April 2013
Accepted 7 April 2013
Available online 25 April 2013
Communicated by A. Pikovsky

Keywords:
Wave localization
Nonlinear dynamics
Chaos
Wave propagation
Subdiffusion
Nonlinear diffusion equation

ABSTRACT

Probably yes, since we find a striking similarity in the spatio-temporal evolution of nonlinear diffusion equations and wave packet spreading in generic nonlinear disordered lattices, including self-similarity and scaling. We discuss, analyze and compare nonlinear diffusion equations with compact or exponentially decaying interactions, and generalized dependences of the diffusion coefficient on the density. Our results strongly support applicability to wave packet spreading in disordered nonlinear lattices.

1. Introduction

The combined impact of disorder and nonlinearity strongly affects the transport properties of many physical systems leading to complex behavior contrary to their separate linear counterparts. The application has great range; particularly relevant are nonlinear effects in cold atoms [1,2], superconductors [3], and optical lattices [4–6]. Yet experimental probing of both disordered and nonlinear media remains limited due to reachable time or size scales.

Significant achievements towards understanding the interplay of disorder and nonlinearity have been made in recent theoretical and numerical studies. A highly challenging problem was the dynamics of compact wave packets expanding in a disordered potential, in the presence of nonlinearity. The majority of studies focused on two paradigmatic models – the discrete nonlinear Schrödinger (DNLS) and the Klein–Gordon (KG) equations – revealing both destruction of an initial packet localization and its resulting subdiffusive spreading, however with debate regarding the asymptotic spreading behaviors [7–14]. Hypotheses of an ultimate slowing-down [15,16] or eventual blockage of spreading [17,18] have been recently challenged with evidence in [19], which reported a finite probability of unlimited packet expansion, even for small nonlinearities. For more details on ongoing controversial debates, we refer the reader to the recent review [20]. A qualitative theory of the nonlinear wave evolution in disordered media is based on the random phase ansatz [12], derives power-law dependences of the diffusion coefficient on the local densities, and predicts several distinct regimes of subdiffusion that match numerics [11–14] convincingly. Closely tied to these phenomena is thermal conductivity in a disordered quartic KG chain, analyzed in [21].

Similar power-law dependences of the diffusion coefficient on the local density have been extensively studied in the context of the nonlinear diffusion equation (NDE). The NDE universally

* Corresponding author.
E-mail address: lapteva@pks.mpg.de (T.V. Laptyeva).

0167-2789/$ – see front matter © 2013 Elsevier B.V. All rights reserved.
http://dx.doi.org/10.1016/j.physd.2013.04.005

describes a diverse range of different phenomena, such as heat transfer, fluid flow or diffusion. It applies to gas flow through porous media [22,23], groundwater infiltration [24,25], or heat transfer in plasma [26]. As a key trait, the NDE admits self-similar solutions (also known as the source-type solution, ZKB solution or Barenblatt–Pattle solution). It describes the diffusion from a compact initial spot and was first studied by Zel'dovich, Kompaneets, and Barenblatt [27,28].

The connection between nonlinear disordered spatial wave equations and NDE was conjectured recently and remains an open terrain [29,15,30–33]. A particularly challenging question is whether the NDE self-similar solution is an asymptotic time limit for the wave packet spreading in nonlinear disordered arrays. If yes, this will support the expectations that compact wave packets spread indefinitely, without re-entering Anderson localization. In this paper, we demonstrate that the NDE captures essential features of energy/norm diffusion in nonlinear disordered lattices. At present, we still lack a rigorous derivation of the NDE from the Hamiltonian equations for nonlinear disordered chains. Here we show that at a sufficiently large time the properties of the NDE self-similar solution reasonably approximate those of the energy/norm density distribution of nonlinear waves; manifesting in similar asymptotical behaviors of statistical measures (such as distribution moments and kurtosis), and in the overall scaling of the density profiles. To substantiate our conclusions, we perform simulations of a modified NDE and compare the results against the spatio-temporal evolution of nonlinear disordered media [13,14].

2. Theoretical predictions

2.1. Basic nonlinear disordered models

The spreading of wave packets has been extensively studied within the framework of KG/DNLS arrays. Particularly, the DNLS describes the wave dynamics in various experimental contexts, from optical wave-guides [5,6] to Bose–Einstein condensates [34]. It was found that the KG equation approximates well the DNLS one under appropriate conditions of small energy densities. This is substantiated by previous derivations of the correspondence in the ordered lattice case [35,36]. While a similar derivation for the disordered case is missing, an enormous amount of numerical data shows that the analogy is working for the spreading characteristics of wave packets [10,11,13,14]. We perform computations exactly in the same parameter regimes covered by these previous studies. Note also that the KG has the advantage of faster integration at the same level of accuracy.

The DNLS chain is described by the equations of motion

$$i\dot{\psi}_l = \epsilon_l \psi_l + \beta |\psi_l|^2 \psi_l - \psi_{l+1} - \psi_{l-1}, \tag{1}$$

where ϵ_l is the potential strength on the site l, chosen uniformly from an uncorrelated random distribution $[-W/2, W/2]$ parameterized by the disorder strength W.

The KG lattice is determined by

$$\ddot{u}_l = -\tilde{\epsilon}_l u_l - u_l^3 + \frac{1}{W}(u_{l+1} + u_{l-1} - 2u_l), \tag{2}$$

where u_l and p_l are, respectively, the generalized coordinate/momentum on the site l with an energy density E_l. The disordered potential strengths $\tilde{\epsilon}_l$ are chosen uniformly from the random distribution $[1/2, 3/2]$. The total energy $\bar{E} = \sum_l E_l$ acts as the nonlinear control parameter, analogous to β in DNLS (see e.g. [11]).

Both models conserve the total energy, the DNLS additionally conserves the total norm $S = \sum_l |\psi_l|^2$. The approximate mapping from the KG to the DNLS is $\beta S \approx 3W\bar{E}$ was empirically confirmed in a large number of extensive numerical simulations [10–14]. Therefore we restrict analytics to the DNLS model. We also note that we exclude here numerical considerations for strong nonlinearities where self trapping occurs in the DNLS model rigorously due to the two integrals of motion [17]. For the KG a similar theorem does not exist (note however that again previous numerical investigations [10–14] showed that self trapping occurs in the KG case as well up to the largest computed times).

2.1.1. Spreading predictions

In order to quantitatively characterize the wave-packet spreading in Eqs. (1) and (2) and compare the outcome to the NDE model, we track the probability at the l-th site, $\mathcal{P}_l \equiv n_l = |\psi_l|^2$, where n_l is the norm density distribution. Note that the analog of n_l in the KG is the normalized energy density distribution E_l. We then track a normalized probability density distribution, $z_l \equiv n_l / \sum_k n_k$. In order to probe the spreading, we compute the time-dependent moments $m_\eta = \sum_l z_l (l - \bar{l})^\eta$, where $\bar{l} = \sum_l l z_l$ gives the distribution center.

We further use as an additional dynamical measure the kurtosis [37], defined as $\gamma(t) = m_4(t)/m_2^2(t) - 3$. Kurtosis is an indicator of the overall shape of the probability distribution profile—in particular, as a deviation measure from the normal profile. Large values correspond to profiles with sharp peaks and long extending tails. Low values are obtained for profiles with rounded/flattened peaks and steeper tails. As an example, the Laplace distribution has $\gamma = 3$, while a compact uniform distribution has $\gamma = -1.2$.

The time dependence of the second moment m_2 of the above distributions z_l was previously derived and studied in [10–14]. Different regimes of energy/norm subdiffusion were observed and explained. Generally, m_2 follows a power-law t^α with $\alpha < 1$. Here we briefly recall the key arguments.

In the linear limit Eqs. (1) and (2) reduce to the same eigenvalue problem [10,11]. We can thus determine the normalized eigenvectors $A_{\nu,l}$ and the eigenvalues λ_ν. With $\psi_l = \sum_\nu A_{\nu,l}\phi_\nu$, Eq. (1) reads in an eigenstate basis as

$$i\dot{\phi}_\nu = \lambda_\nu \phi_\nu + \beta \sum_{\nu_1,\nu_2,\nu_3} I_{\nu,\nu_1,\nu_2,\nu_3} \phi^*_{\nu_1} \phi_{\nu_2} \phi_{\nu_3}, \tag{3}$$

where $I_{\nu,\nu_1,\nu_2,\nu_3} = \sum_l A_{\nu,l} A_{\nu_1,l} A_{\nu_2,l} A_{\nu_3,l}$ are overlap integrals and ϕ_ν determine the complex time-dependent amplitudes of the eigenstates.

In [12] the incoherent "heating" of cold exterior by the packet has been established as the most probable mechanism of spreading. Following this analysis, the packet modes $\phi_\nu(t)$ should evolve chaotically with a continuous frequency spectrum. In particular, chaotic dynamics of phases is expected to destroy localization. The degree of chaos is linked to the number of resonances, whose probability becomes an essential measure for the spreading. Previous studies [38] indicate that the probability of a packet eigenstate to be resonant is $\mathcal{R}(\beta n) = 1 - e^{-C\beta n}$, with C being a constant dependent on the strength of disorder. The heating of an exterior mode close to the edge of the wave packet with norm density n would then follow

$$i\dot{\phi}_\mu = \lambda_\mu \phi_\mu + \beta n^{3/2} \mathcal{R}(\beta n) f(t) \tag{4}$$

with delta-correlated (or, reasonably, short-time correlated) noise $f(t)$, and lead to $|\phi_\mu|^2 \sim \beta^2 n^3 (\mathcal{R}(\beta n))^2 t$. The momentary diffusion rate follows as $D \sim \beta^2 n^2 (\mathcal{R}(\beta n))^2$.

With $m_2 \sim n^{-2} = Dt$ one arrives at $1/n^2 \sim \beta(1 - e^{-C\beta n}) t^{1/2}$. Depending on the product $C\beta n$ being larger or smaller than one, the packet has two regimes of subdiffusion (and a dynamical crossover between them): $m_2 \sim \beta t^{1/2}$ (strong chaos) and $m_2 \sim \beta^{4/3} t^{1/3}$ (asymptotic weak chaos) [10–14].

The validity of the assumption of incoherent phases and of Eq. (4) was established through numerical studies for the first time by Michaely and Fishman [39], moving the above conjecture based theories onto solid grounds.

2.2. Nonlinear diffusion equation

The assumption of chaos and random phases, Eq. (4), the density dependent diffusion coefficient and the resulting subdiffusion strongly suggest an analogy to nonlinear diffusion equations (see e.g. Ref. [40]). We first consider here the much studied NDE with a power-law dependence of the diffusion coefficient on the density. The NDE in the one-dimensional case reads

$$\partial_t \mathcal{P} = \partial_x \left(\kappa \mathcal{P}^a \partial_x \mathcal{P}\right). \tag{5}$$

Here $\mathcal{P} \equiv \mathcal{P}(x,t)$ is the concentration of the diffusing species (which may be related to the energy/norm density), $a > 0$ and κ are some constants. Hereafter, we set $\kappa = 1$ without loss of generality.

The NDE conserves one quantity – its total norm. It appears therefore to be well suited for the KG model, which also conserves one quantity – the total energy. The NDE can be thus expected to describe diffusion of energy in the KG model. However, the DNLS model conserves two quantities. Is therefore a more complicated two-component NDE type equation needed in that case? Apparently, not necessarily when wave packet spreading into an empty (zero densities) volume is studied. This follows from the proportionality of energy and norm density currents for DNLS in the limit of small densities, and is further supported by our numerics. Further support comes from the studies of Mulansky et al., where a number of comparisons between the NDE and the DNLS dynamics were performed [29]. It remains an interesting open question, at which levels of the complicated nonlinear dynamics this difference in the number of conserved quantities begins to matter.

Let us discuss the scaling properties of Eq. (5). Given a solution $\mathcal{P}(x,t)$ it follows that

$$\mathcal{P}(x,t) = s_p \mathcal{P}(s_x x, s_t t), \tag{6}$$

where s_p, s_x, s_t are some scaling factors. From normalization it follows that $s_p = s_x$. Inserting (6) into (5) we find

$$s_t = s_x^{a+2}. \tag{7}$$

After some algebra for the moment $m_\eta(t)$ we conclude

$$m_\eta = \left(\frac{t}{t_0}\right)^{\eta/(a+2)} m_\eta(t_0), \tag{8}$$

which corresponds to a subdiffusive process.

Eq. (5) has various self-similar solutions [41,42,25], which depend on the characteristics of the evolving state. For compact wave packets, the self-similar state is realized in the asymptotic limit of large time [27,28,43]:

$$\mathcal{P}(x,t) = \left[A - \frac{a x^2}{2(2+a)t^{2/(2+a)}}\right]^{1/a} t^{-1/(2+a)}, \tag{9}$$

where A is a normalization constant and $|x| < x_0$. For $|x| > x_0$ the density $\mathcal{P}$ strictly vanishes. The edge position x_0 depends on time as

$$x_0 = \left[2A(2/a+1)t^{2/(2+a)}\right]^{1/2}. \tag{10}$$

The linear stability of Eq. (9) was demonstrated in [44,45].

Using a change of variables $y = x/x_0$, we obtain for the density $\bar{\mathcal{P}}(y,t)$ with $\bar{\mathcal{P}}\mathrm{d}y = \mathcal{P}\mathrm{d}x$:

$$\bar{\mathcal{P}}(y,t) = A^{1/a+1/2}\sqrt{4/a+2}(1-y^2)^{1/a}. \tag{11}$$

Since $\bar{\mathcal{P}}$ does not depend on time, it follows

$$m_\eta(t) = x_0^\eta \bar{m}_\eta, \quad \bar{m}_\eta = \int_{-1}^{1} y^\eta \bar{\mathcal{P}} dy. \tag{12}$$

In agreement with (8) this yields e.g. $m_2 \sim t^{2/(2+a)}$.

The moments of solution (9) are

$$m_\eta = \left[\frac{2(2+a)}{a}\right]^{\frac{\eta+1}{2}} \mathcal{B}\left[\frac{a+1}{a}, \frac{\eta+1}{2}\right] A^{\frac{a(\eta+1)+2}{2a}} t^{\frac{\eta}{2+a}}, \tag{13}$$

where $\mathcal{B}[x,y]$ is the Euler Beta Function. Using Eq. (13), we derive for the kurtosis

$$\gamma_\infty \equiv \lim_{t\to\infty}\gamma = 3\frac{\Gamma\left[\frac{5}{2}+\frac{1}{a}\right]\Gamma\left[\frac{5}{2}+\frac{1}{a}\right]}{\Gamma\left[\frac{3}{2}+\frac{1}{a}\right]\Gamma\left[\frac{7}{2}+\frac{1}{a}\right]} - 3, \tag{14}$$

where $\Gamma[x]$ is Legendre's Gamma function. As can be seen, the kurtosis of the self-similar solution does not depend on time. For the values $a = 4$ and $a = 2$ we obtain kurtosis values $\gamma = -1.091$ and $\gamma = -1.00$ respectively. Additionally, $\gamma = -1.20$ in the limit of $a \to \infty$, which corresponds to a flat uniform distribution.

A few remarks are required in order to proceed. First, the spatial discretization of the NDE (5) by introducing discrete Laplacians with nearest-neighbor differences does not modify the properties of the asymptotic states [40]. However, the overlap integrals in (3) decay exponentially in space. Therefore spreading wave packets will have exponentially decaying tails, instead of being compact as it happens in the NDE. Moreover, the diffusion coefficient D for spreading wave packets is in general different from a pure power of the density (see Eq. (4) and below). It takes such a power function form only in the asymptotic regime of weak chaos and the potentially long-lasting intermediate strong chaos regime. Therefore, we will generalize and adapt the above NDE in the next subsection.

2.3. Modified nonlinear diffusion equation

Firstly, we rewrite Eq. (5) as

$$\partial_t \mathcal{P} = \frac{1}{a+1}\partial_x^2 \mathcal{P}^{a+1}. \tag{15}$$

Since density leakage into neighboring sites is directly related to resonance probability [10–14], we introduce it into the RHS of Eq. (15) following the discussion of Eq. (4) as

$$\mathcal{P}^{a+1} \to F = \mathcal{P}^{a+1}\left(1 - e^{-C\mathcal{P}}\right)^2.$$

Randomness in disordered systems exponentially localizes the normal modes, so mode–mode coupling in the nonlinear overlap integral has an exponential dependence in distance as well. We therefore introduce an exponentially decaying interaction along a discrete chain. Using a finite central difference, we arrive at the modified nonlinear diffusion equation (MNDE):

$$\partial_t \mathcal{P}_n = \sum_{m>n} e^{-m/\chi}\left(F_{n-m} - 2F_n + F_{n+m}\right). \tag{16}$$

The parameter χ is corresponding to the localization length. In the above, we treat C as a free parameter, and equal χ in our numerics to localization lengths of the disordered lattice models. We choose $a = 2$ for the MNDE in order to obtain the proper correspondence to the wave packet spreading properties (see Eq. (4) and discussion), and expect to observe similar regimes, such that with $\mathcal{P}_l \sim 1$ we have weak chaos for $C \ll 1$ and strong chaos in the opposite limit of $C \gg 1$. The above MNDE is therefore expected to account for the resonance probabilities between normal modes, and the exponentially decaying interaction between them.

The exponentially decaying interactions in (16) can be expected to lead to a loss of the scaling properties of the MNDE as compared to the NDE. However, asymptotically the same scaling laws could again still hold for the following reason. In the NDE for large times the length scales increase as well. The exponential decay of interactions in the MNDE is controlled by the localization length of

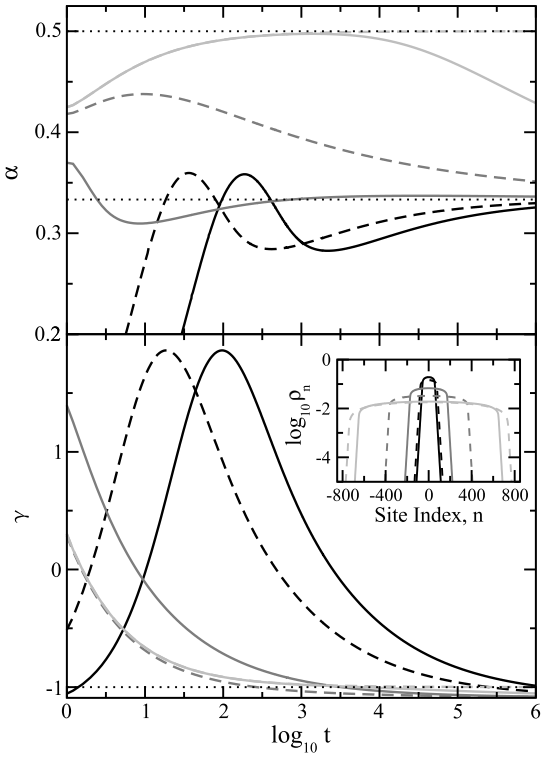

Fig. 1. Numerical results for the MNDE with $\chi = 6$ and $a = 2$, for initial conditions given in the text. *Upper:* The exponent $\alpha(t)$ for the MNDE with the following values of C: 0.1 (dashed black), 1.0 (solid black), 10 (dashed dark gray), 25 (solid dark gray), 50 (dashed light gray), and 10^3 (solid light gray). *Lower:* The kurtosis $\gamma(t)$ for the same simulations. *Inset:* The density profiles of the above simulations at $t = 10^6$.

the underlying linear wave equation, which stays finite. As soon as the NDE length scales become large enough, they coarse grain over the much shorter localization length, and we can expect a wave packet profile, which restores the scaling features of the NDE in its central part, yet keeping exponential tails, which do not follow the NDE scaling. As we will see below, this is indeed what we observe.

2.4. Numerical simulations of MNDE

We integrate Eq. (16) with a fourth-order Runge–Kutta scheme [46], for a number of values for the free parameter C. We start with an initially compact distribution of width $L = 41$ and density $\mathcal{P}_{|l|\leq L/2} = 1$ (hereafter referred to as a *brick* distribution) and $\mathcal{P}_{|l|>L/2} = 0$. The integrations were carried out to $t \approx 10^6$ using a time step of 0.4, all the while conserving norm to better than 10^{-12}.

From the second moment, $m_2(t)$, we compute the derivative

$$\alpha(t) = \frac{\mathrm{d}\log_{10} m_2}{\mathrm{d}\log_{10} t} \tag{17}$$

and plot the result in the upper panel of Fig. 1. We find that the MNDE reproduces weak chaos ($\alpha = 1/3$ for $C \leq 1$) and intermediate strong chaos ($\alpha = 1/2$ for $C \gg 1$).

We further plot in Fig. 1 the time-dependent kurtosis (lower panel) and the density distributions at $t = 10^6$ (inset), for a few representative values of C. Note that those states that are in the weak chaos regime ($C \lesssim 1$) show a tendency towards an asymptotic $\gamma_\infty \approx -1.091$ in agreement with the NDE, but not reaching it fully in our simulations. Those states in the intermediate strong chaos regime ($C \gtrsim 100$) exhibit long-lasting saturation at $\gamma_\infty \approx -1$ in agreement with the NDE. We also observe a growth of the kurtosis into positive values for weak chaos, followed by a drop that decays to -1.091.

3. Wave packet spreading in nonlinear disordered lattices

Let us discuss first the details of computations. For both models of Eqs. (1) and (2) we consider initial brick distributions of width L with nonzero internal energy density (or norm density for the DNLS) and zero outside this interval. In contrast to the NDE and MNDE, these lattice systems (in addition to local densities) are also characterized by local phases. Initially the phase at each site is set randomly. Equations were evolved using SABA-class split-step symplectic integration schemes [47], with time-steps of 10^{-2}–10^{-1}. Energy conservation is within a relative tolerance of less than 0.1%. We perform ensemble averaging over 10^3 realizations of the onsite disorder.

With $m_2 \sim t^{2/(2+a)}$ of the NDE self-similar solution, Eq. (13), and $m_2 \sim t^\alpha$ for KG/DNLS models, the NDE parameter a is related to the exponent α as $a = 2(1-\alpha)/\alpha$. This allows a monitoring of a as the energy density changes. We expect then $a = 2$ and $a = 4$ respectively for the strong and weak chaos regimes, as well as a shift from $a = 2$ to $a = 4$ associated with the crossover between the two regimes.

We validate these predictions using our numerical data that correspond to the different regimes of spreading [13]. We plot in Fig. 2 the NDE parameter a from the numerically obtained α (see inset in Fig. 2), assuming that the energy density $E(t) \sim E(0)L\,\langle m_2(t)\rangle^{-1/2}$. As predicted, a reaches the asymptotic value $a = 4$ for weak chaos. Our numerical results also show that once a reaches its asymptotic value $a = 4$, it does not increase further in time, even for quite small energy densities. That is a clear indication for the absence of speculated slowing-down dynamics [15]. For strong chaos, a temporarily saturates around $a = 2$, keeps this value only within some interval of energy densities, and finally crosses over into the interval $2 < a < 4$ with a clear tendency to reach the weak chaos value $a = 4$ at larger times.

The resulting kurtosis evolution $\langle\gamma(t)\rangle$ is presented in Fig. 3. For the initial wave packet $\langle\gamma(0)\rangle = -1.2$. The kurtosis first displays a transient increase to positive values. This is very similar to the MNDE results and is due to exponential localization of the initial state in normal mode space. At larger times $\langle\gamma(t)\rangle$ displays a decrease in time, approaching the self-similar behaviors in density distributions with $\langle\gamma\rangle \approx -1$ (recall that the NDE self-similar solution gives us $\gamma = -1$ for $a = 2$ and $\gamma = -1.091$ for $a = 4$).

The evolution of the averaged energy density profiles $\langle E\rangle$ in the course of spreading is illustrated in Fig. 4. The peaked initial distribution profiles transform into more flat ones as time evolves. The most striking result is obtained by rescaling the profiles in Fig. 4 according to the scaling laws of the NDE. We estimate the value of x_0 (see Eq. (10)) as the distance between the position where the profiles in Fig. 4 reach 10^{-4} and the center of the wave packet $l = 500$. We then plot the rescaled densities according to Eq. (11) in the inset of Fig. 4. This is obtained by rescaling the coordinate $(l - 500) \to (l - 500)/x_0$ and rescaling the whole distribution function $z_l \to x_0 z_l$. In practical terms we simply rescale the curves for $t = 10^4$ and $t = 10^7$ to coincide with the curve at $t = 10^8$ and then stretch the rescaled curves to extend from $l = 0$ to $l = 1000$. We observe very good scaling behavior.

To make sure that the scaling is not just a property of the KG model, we perform the scaling also with data for the DNLS. We take $\beta = 0.04$ and the data already used in Fig. 3. We show in Fig. 5 the corresponding data for the times $t = 10^5, 10^6, 10^7$ and rescale them similar to the KG case. The result is shown in the inset of Fig. 5 and shows again very good agreement.

Together with the proper scaling of x_0 which was tested in [29], this is the strongest argument to support the applicability of NDE and MNDE to the spreading of wave packets in nonlinear disordered systems. It also strongly supports that the spreading process follows the predicted asymptotics and does not slow down or even halt.

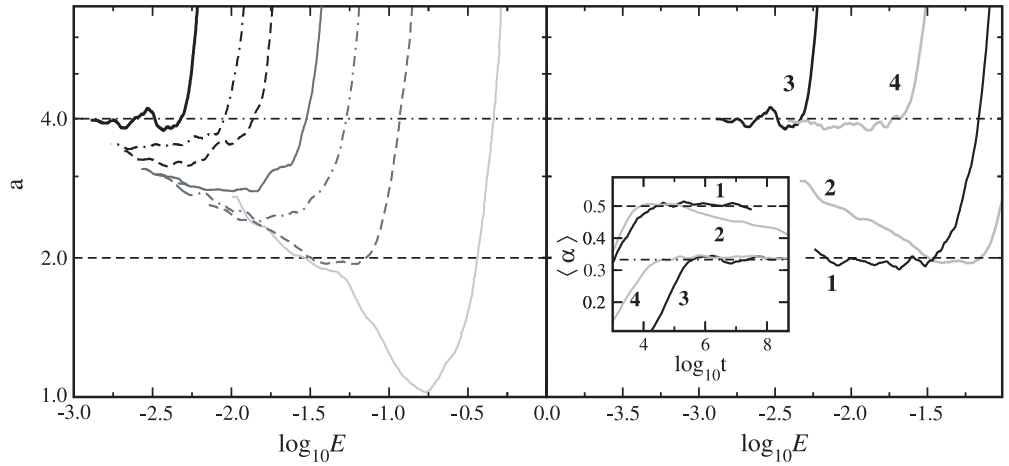

Fig. 2. The NDE parameter a versus the energy density $E(t) \sim E(0)L\,\langle m_2(t)\rangle^{-1/2}$ as obtained from numerical simulations of the KG chain. Horizontal lines guide the eye at values $a = 2$ and $a = 4$. *Left panel*: $W = 4$, $L = 21$, and $E \in \{0.01, 0.02, 0.03, 0.06, 0.1, 0.2, 0.75\}$ (varying from the top to bottom and from weak chaos to strong chaos and self trapping). *Right panel*: $W = 2$ and $E = 0.1$ (curve 1, strong chaos), $W = 4$ and $E = 0.2$ (curve 2, crossover from the strong to weak chaos), $W = 4$ and $E = 0.01$ (curve 3, weak chaos), $W = 6$ and $E = 0.05$ (curve 4, weak chaos). *Inset*: Dependence of α on time for the same data as in the right panel. The dot-dashed and dashed lines correspond to the values $\alpha = 1/3$ and $\alpha = 1/2$ respectively.

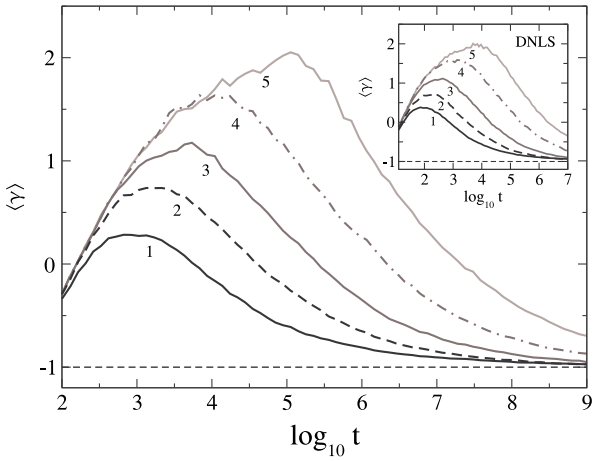

Fig. 3. Semi-log plot of average over 10^3 realizations kurtosis $\langle\gamma\rangle$ versus time for KG (see main part) and DNLS (see inset) models with parameters $W = 4$, $L = 21$. Numbers correspond to different energy densities (KG), or, nonlinearity strengths (DNLS): $E = 0.01$ or $\beta = 0.04$ (curve 5), $E = 0.02$ or $\beta = 0.08$ (curve 4), $E = 0.04$ or $\beta = 0.18$ (curve 3), $E = 0.08$ or $\beta = 0.36$ (curve 2), $E = 0.2$ or $\beta = 0.72$ (curve 1). The dashed lines correspond to the $\langle\gamma\rangle = -1.0$.

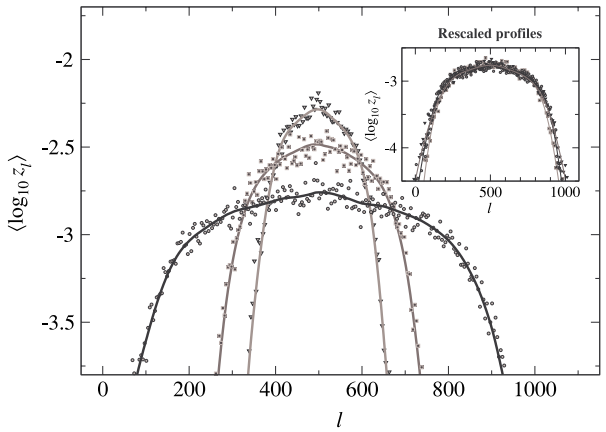

Fig. 4. KG: the log of the normalized energy density distribution $\langle\log_{10} z_l\rangle$ at three different times (from top to bottom $t \approx 10^4, t \approx 10^7, t \approx 10^8$). The initial parameters are $E = 0.2, W = 4$ and $L = 21$. Symbols correspond to the average over 10^3 disorder realizations, and solid lines correspond to an additional smoothing. *Inset:* Rescaled distributions (see text).

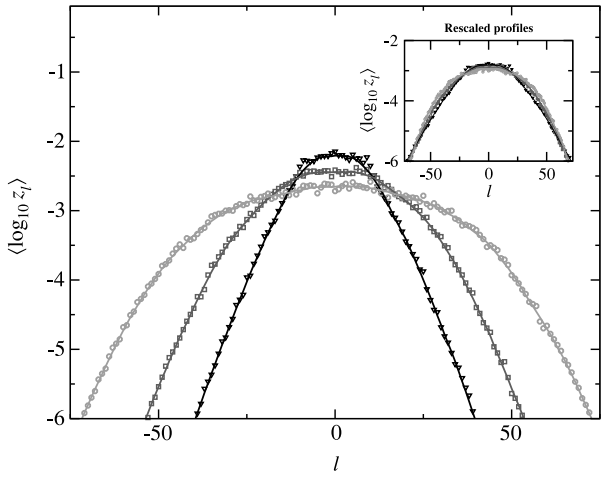

Fig. 5. DNLS: the log of the normalized norm density distribution $\langle\log_{10} z_l\rangle$ at three different times (from top to bottom $t \approx 10^5, t \approx 10^6, t \approx 10^7$). The initial parameters are $\beta = 0.04, W = 4$, and $L = 21$. Symbols correspond to the average over 10^3 disorder realizations, and solid lines correspond to an additional smoothing. *Inset:* Rescaled distributions (see text).

4. Conclusion

We scrutinized the suggested connection between the temporal evolution of self-similar solutions of the NDE and MNDE on one side, and the asymptotic dynamics of the energy/norm distribution within nonlinear disordered media on the other, and found a remarkable correspondence. In order to describe the expansion of an initial distribution with time, we used two key quantities: (i) the second moment $m_2(t)$, which shows how the squared width of the distribution grows; (ii) the kurtosis $\gamma(t)$, which indicates how the shape of the distribution profile changes.

As a first test we compared the exponents characterizing the subdiffusion for the second moments of the energy/norm density distributions. In KG/DNLS models, $m_2(t) \sim t^{\alpha}$, and for the NDE self-similar solution, $m_2(t) \sim t^{2/(2+a)}$, the exact identity giving $\alpha = 2/(2 + a)$. We found that the wave packets in nonlinear disordered chains converge towards the self-similar behavior at large times. The numerical results show a good correspondence to the NDE-based analytics in a wide range of parameters.

Second, in disordered lattices the energy/norm distributions have exponentially decaying tails at variance to the steep-edged

NDE self-similar solution. Such a difference of energy/norm distribution profiles has no effect on $m_2(t)$ at large times. However, it leads to differences between the NDE and the KG/DNLS dynamics at intermediate times, e.g. seen in the temporal behavior of the kurtosis $\langle\gamma(t)\rangle$. In order to study the possible impact of various initial density profiles, we also computed the time evolution of the NDE for initial probability distributions with exponential tails. In all simulations with NDE parameter $a \leq 6$, the kurtosis asymptotically reached the expected value γ_∞ being a function of the parameter a only.

To bridge a possible gap between the NDE and the disordered nonlinear lattices, we introduced a modified MNDE. To account for the interaction between localized Anderson lattice modes we implemented exponentially decaying coupling in the MNDE, and also incorporated the resonance probability of normal modes into a modified nonlinear diffusion coefficient. Then we indeed observe the dynamical behavior that reproduces the spatio-temporal evolution of nonlinear disordered chains, namely the weak and the strong chaos regimes of spreading, and we correct temporal evolution of the kurtosis, and the distribution profiles. Most importantly we observe the precise scaling behavior of the asymptotic NDE solutions in the case of nonlinear wave packets.

Let us summarize. There is a lack of knowledge on the statistical properties of chaotic dynamics generated by nonlinear coupling. We are still far from a rigorous derivation of the NDE when starting with the equations of motion for nonlinear disordered chains. Nevertheless, the theory for initial energy/norm spreading in KG/DNLS chains which is based on a Langevin dynamics approximation has earlier been confirmed by exhaustive numerical studies. Of course, there is difference between KG/DNLS nonlinear disordered models and the NDE. Despite this, numerical results confirm that at sufficiently large time the NDE self-similar solution approximates remarkably well the spreading properties of energy/norm density distributions in terms of the second moment, the kurtosis, and the scaling features. Therefore, the NDE as a simple analytical tool is extremely useful for studying the initial excitation spreading in nonlinear disordered media at asymptotically large times. Additionally, the NDE analog with long-range exponentially decaying coupling shows an even deeper correspondence between generic nonlinear disordered models and the NDE and therefore might prove to be an insightful model for the future analysis of spreading in nonlinear disordered systems.

Acknowledgments

We thank N. Li, M.V. Ivanchenko, and G. Tsironis for insightful discussions.

References

[1] E. Lucioni, B. Deissler, L. Tanzi, et al., Observation of subdiffusion in a disordered interacting system, Phys. Rev. Lett. 106 (2011) 230403.
[2] S.E. Pollack, D. Dries, R.G. Hulet, et al., Collective excitation of a Bose–Einstein condensate by modulation of the atomic scattering length, Phys. Rev. A 81 (2010) 053627.
[3] Y. Dubi, Y. Meir, Y. Avishai, Nature of the superconductor-insulator transition in disordered superconductors, Nature 449 (2007) 876–880.
[4] T. Pertsch, U. Peschel, J. Kobelke, et al., Nonlinearity and disorder in fiber arrays, Phys. Rev. Lett. 93 (2004) 053901.
[5] T. Schwartz, G. Bartal, S. Fishman, M. Segev, Transport and Anderson localization in disordered two-dimensional photonic lattices, Nature 446 (2007) 52–55.
[6] Y. Lahini, A. Avidan, F. Pozzi, et al., Anderson localization and nonlinearity in one-dimensional disordered photonic lattices, Phys. Rev. Lett. 100 (2008) 013906.
[7] M.I. Molina, Transport of localized and extended excitations in a nonlinear Anderson model, Phys. Rev. B 58 (1998) 12547.
[8] D.L. Shepelyansky, Delocalization of quantum chaos by weak nonlinearity, Phys. Rev. Lett. 70 (1993) 1787–1790.
[9] A.S. Pikovsky, D.L. Shepelyansky, Destruction of Anderson localization by a weak nonlinearity, Phys. Rev. Lett. 100 (2008) 094101.
[10] S. Flach, D.O. Krimer, Ch. Skokos, Universal spreading of wave packets in disordered nonlinear systems, Phys. Rev. Lett. 102 (2009) 024101.
[11] Ch. Skokos, D.O. Krimer, S. Komineas, S. Flach, Delocalization of wave packets in disordered nonlinear chains, Phys. Rev. E 79 (2009) 056211.
[12] S. Flach, Spreading of waves in nonlinear disordered media, Chem. Phys. 375 (2010) 548–556.
[13] T.V. Laptyeva, J.D. Bodyfelt, Ch. Skokos, et al., The crossover from strong to weak chaos for nonlinear waves in disordered systems, Europhys. Lett. 91 (2010) 30001.
[14] J.D. Bodyfelt, T.V. Laptyeva, Ch. Skokos, et al., Nonlinear waves in disordered chains: probing the limits of chaos and spreading, Phys. Rev. E 84 (2011) 016205.
[15] M. Mulansky, K. Ahnert, A. Pikovsky, Scaling of energy spreading in strongly nonlinear disordered lattices, Phys. Rev. E 83 (2011) 026205.
[16] A. Pikovsky, S. Fishman, Scaling properties of weak chaos in nonlinear disordered lattices, Phys. Rev. E 83 (2011) 025201.
[17] G. Kopidakis, S. Komineas, S. Flach, S. Aubry, Absence of wave packet diffusion in disordered nonlinear systems, Phys. Rev. Lett. 100 (2008) 084103.
[18] M. Johansson, G. Kopidakis, S. Aubry, KAM tori in 1D random discrete nonlinear Schrödinger model? Europhys. Lett. 91 (2010) 50001.
[19] M.V. Ivanchenko, T.V. Laptyeva, S. Flach, Anderson localization or nonlinear waves: a matter of probability, Phys. Rev. Lett. 107 (2011) 240602.
[20] S. Fishman, Y. Krivolapov, S. Soffer, The nonlinear Schrödinger equation with a random potential: results and puzzles, Nonlinearity 25 (2012) R53.
[21] S. Flach, M.V. Ivanchenko, N. Li, Thermal conductivity of nonlinear waves in disordered chains, Pramana J. Phys. 77 (2011) 1007.
[22] L.S. Leibenzon, The motion of a gas in a porous medium, Complete Works of Acad. Sciences, URSS, 1930.
[23] M. Muskat, The Flow of Homogeneous Fluids Through Porous Media, McGraw-Hill, New York, 1937.
[24] J. Boussinesq, Recherches théoriques sur l'écoulement des nappes d'eau infiltrés dans le sol et sur le débit des sources, J. Math. Pures Appl. 10 (1904) 5–78.
[25] W.F. Ames, Nonlinear Partial Differential Equations in Engineering, Academic, New York, 1965.
[26] Y.B. Zel'dovich, Y.P. Raizer, Physics of Shock Waves and High-Temperature Hydrodynamic Phenomena, Academic Press, New York, 1966.
[27] Y.B. Zel'dovich, A. Kompaneets, Collected Papers of the 70th Anniversary of the Birth of Academician A. F. Ioffe, Moscow, 1950.
[28] G.I. Barenblatt, On some unsteady motions of a liquid and gas in a porous medium, Prikl. Mat. Mekh. 16 (1952) 67–78.
[29] M. Mulansky, A. Pikovsky, Spreading in disordered lattices with different nonlinearities, Europhys. Lett. 90 (2010) 10015.
[30] V.M. Kenkre, D.K. Campbell, Self-trapping on a dimer: time-dependent solutions of a discrete nonlinear Schrödinger equation, Phys. Rev. B 34 (1986) 4959.
[31] N. Cherroret, T. Wellens, Fokker–Planck equation for transport of wave packets in nonlinear disordered media, Phys. Rev. E 84 (2011) 021114.
[32] G. Schwiete, A.M. Finkel'stein, Nonlinear wave-packet dynamics in a disordered medium, Phys. Rev. Lett. 104 (2010) 103904.
[33] G. Schwiete, A.M. Finkel'stein, An effective theory of pulse propagation in a nonlinear and disordered medium in two dimensions, in: A. Aharony, O. Entin-Wohlman (Eds.), Perspectives of Mesoscopic Physics—Dedicated to Yoseph Imry's 70th Birthday, World Scientific Publishing Co., Singapore, 2010, pp. 249–264.
[34] A. Smerzi, A. Trombettoni, Discrete nonlinear dynamics of weakly coupled Bose–Einstein condensates, Chaos 13 (2003) 766.
[35] Y. Kivshar, M. Peyrard, Modulational instabilities in discrete lattices, Phys. Rev. A 46 (1992) 3198–3205.
[36] M. Johansson, Discrete nonlinear Schrödinger approximation of a mixed Klein–Gordon/Fermi–Pasta–Ulam chain: modulation instability and a statistical condition for creation of thermodynamic breathers, Physica D 216 (2006) 62–70.
[37] Y. Dodge, The Oxford Dictionary of Statistical Terms, sixth ed., Oxford University Press, New York, 2003.
[38] D.O. Krimer, S. Flach, Statistics of wave interactions in nonlinear disordered systems, Phys. Rev. E 82 (2010) 046221.
[39] E. Michaely, S. Fishman, Effective noise theory for the nonlinear Schrödinger equation with disorder, Phys. Rev. E 85 (2012) 046218.
[40] A.R. Kolovsky, E.A. Gomez, H.J. Korsch, Bose–Einstein condensates on tilted lattices: coherent, chaotic and subdiffusive dynamics, Phys. Rev. A 81 (2010) 025603.
[41] J.L. Vazquez, The Porous Medium Equation: Mathematical Theory, Clarendon Press, Oxford, 2007.
[42] A.D. Polyanin, V.F. Zaitsev, Handbook of Nonlinear Partial Differential Equations, Chapman and Hall/CRC, 2004.
[43] B. Tuck, Some explicit solutions to the non-linear diffusion equation, J. Phys. D: Appl. Phys. 9 (1976) 1559.
[44] T.P. Witelski, A.J. Bernoff, Self-similar asymptotics for linear and nonlinear diffusion equations, Stud. Appl. Math. 100 (1998) 153–193.
[45] J.S. Mathunjwa, A. Hogg, Self-similar gravity currents in porous media: linear stability of the Barenblatt–Pattle solution revisited, Eur. J. Mech. B Fluids 25 (2006) 360–378.
[46] W.H. Press, FORTRAN Numerical Recipes, second ed., Cambridge University Press, New York, 1996.
[47] J. Laskar, P. Robutel, High order symplectic integrators for perturbed Hamiltonian systems, Celestial Mech. Dynam. Astronom. 80 (2001) 39–62.